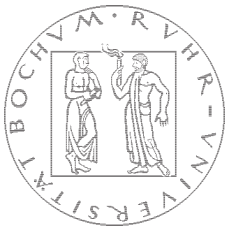

Preprint 01-2008

# An error-estimate-free and remapping-free variational mesh refinement and coarsening method for dissipative solids at finite strains

J. Mosler and M. Ortiz

Ruhr University Bochum
California Institute of Technology

This is a preprint of an article accepted by:

*International Journal for Numerical Methods in Engineering* (2008)

# An error-estimate-free and remapping-free variational mesh refinement and coarsening method for dissipative solids at finite strains

J. Mosler *†

*Institute of Mechanics*
Ruhr University Bochum
*Universitätsstr. 150,D-44780 Bochum, Germany*
E-Mail: mosler@tm.bi.ruhr-uni-bochum.de

M. Oritz*

*Graduate Aeronautical Laboratories*
California Institute of Technology
*Pasadena, CA 91125, USA*
E-Mail: ortiz@aero.caltech.edu

SUMMARY

A variational $h$-adaptive finite element formulation is proposed. The distinguishing feature of this method is that mesh refinement and coarsening are governed by the same minimization principle characterizing the underlying physical problem. Hence, no error estimates are invoked at any stage of the adaption procedure. As a consequence, linearity of the problem and a corresponding Hilbert-space functional framework are not required and the proposed formulation can be applied to highly nonlinear phenomena. The basic strategy is to refine (respectively, unrefine) the spatial discretization locally if such refinement (respectively, unrefinement) results in a sufficiently large reduction (respectively, sufficiently small increase) in the energy. This strategy leads to an adaption algorithm having $O(N)$ complexity. Local refinement is effected by edge bisection and local unrefinement by the deletion of terminal vertices. Dissipation is accounted for within a time-discretized variational framework resulting in an incremental potential energy. In addition, the entire hierarchy of successive refinements is stored and the internal state of parent elements is updated so that no mesh-transfer operator is required upon unrefinement. The versatility and robustness of the resulting variational adaptive finite element formulation are illustrated by means of selected numerical examples.

## 1 INTRODUCTION

In this paper we extend the variational $h$-adaptive finite element formulation proposed by [1] to include adaptive unrefinement in addition to refinement. The fundamental advantages of the approach are as follows: i) The process of mesh refinement and unrefinement is *error-estimate free* and applies to any problem, linear or nonlinear, with solutions in general function spaces not necessarily normed, provided that the problem possesses a minimum variational structure; ii) in inelastic problems involving materials with an evolving internal state, a hierarchical refinement/unrefinement scheme bypasses the need to define mesh-to-mesh transfer, or *remapping*, operators for the internal variables.

A broad range of phenomena in mechanics are governed by minimum principles. For instance, the stable equilibrium configurations of a hyperelastic body minimize the potential energy of the body. For dissipative materials of the elastic-plastic and elastic-viscoplastic type,

*DoE through Caltech's ASC/ASAP Center
†Deutsche Forschungsgemeinschaft (DFG); contract/grant number: Mo 1389/1-1

Ortiz *et al*. [2–5] have shown that the stable equilibrium configurations of a body can be characterized as minimizers of an incremental potential energy derived by means of time-discretization (see also [6, 7] for a further application of these concepts). Recently, Yang *et al.* [8] have extended this variational approach to account for heat conduction and other transport phenomena.

In these problems, the overriding criterion driving all aspects of the solution is the minimization of the incremental potential energy of the body. Thus, if $F(u)$ denotes the incremental potential energy, an approximate solution $u_1$ is *better* than another approximation solution $u_2$, if and only if $F(u_1) < F(u_2)$. Therefore, it is natural to allow the variational principle to drive mesh adaption as well. The concept of using the underlying variational principle to optimize the discretization enjoys a long tradition dating back, at least, to [9, 10], in the special context of two-dimensional linearized elasticity. When applied to the optimal placement of the nodes, or $r$-adaptivity, variational adaptivity is closely connected to configurational force balance [11, 12], a connection that has been recognized only recently [13–19].

In this paper we are concerned with the formulation of variational $h$-adaption strategies for problems in inelasticity in which the variational principle itself drives mesh refinement and unrefinement. In particular, no error estimates are invoked at any stage of the adaption procedure. However, it can be shown that for linear problems having a quadratic potential energy, variational adaption is equivalent to the minimization of the energy-norm error [1, 20]. The basic mesh refinement strategy follows Mosler and Ortiz [1] and is based on edge bisection of simplicial meshes (cf. [21–23]). Starting from a triangulation of the domain, the repeated application of edge bisection operations defines a *net* $V_h$ of linear spaces parameterized by a *directed* index set $A$. The fundamental problem is then to find the absolute minimizers of the energy in the collection of spaces $\{V_h, h \in A\}$.

The new elements considered in this paper are: i) variational $h$-*unrefinement*; and ii) a remapping-free formulation for inelastic materials whose state is characterized by internal variables. In problems concerned with non-proportional loading, the local resolution requirements may change in time or may shift between different regions of the domain of analysis, which naturally calls for a combination of mesh refinement and unrefinement as a basis for adaption. In the presence of inelasticity, these operations are compounded by the need to transfer the internal state from the old mesh to the adapted mesh, an operation also known as *remapping*. For arbitrary unstructured remeshing, mesh-to-mesh transfer operators may be defined variationally (cf. [24, 25]), but the repeated application of those operators, e. g., in the context of explicit dynamics, may result in significant numerical diffusion. This numerical diffusion can hinder the progression of processes of strain localization and result in overly smooth solutions.

Here we propose a hierarchical mesh refinement/unrefinement strategy for problems of inelasticity that is strictly local and entirely avoids remapping of internal variables, thus eliminating that source of numerical diffusion. In essence, the strategy consists of keeping in storage parent elements that have been refined by edge-bisection and updating their respective internal variables in accordance with the displacement field of the refined mesh. While the state of the parent elements is continually updated, they do not contribute to the internal force vector of the model. Subsequently, unrefinement is effected simply by removing child elements and replacing them by their parent element, whose state is up-to-date. In this manner, a transfer operator of the internal variables is not required upon unrefinement.

The present paper is organized as follows: Section 2 presents a concise review of variational constitutive updates. Within this framework, the deformation mapping follows from minimizing an incremental potential-energy functional that accounts for both energy and dissipation. The edge-bisection operations used to effect refinement/unrefinement are briefly described in the introduction of Section 3. The variational coarsening strategy is presented in Subsection 3.1. An approximate local $O(N)$ adaption criterion is derived in Subsection 3.2. Section 3 is com-

pleted by methods necessary for managing the history variables in case of mesh refinement and coarsening (Subsection 3.3). Finally, the performance of the resulting adaptive finite element formulation is demonstrated in Section 4 by means of selected numerical examples.

# 2 VARIATIONAL FORMULATION OF INELASTIC CONSTITUTIVE UPDATES

The fundamental concept behind variational adaptivity is to rely on the governing variational principle for purposes of optimizing the discretization. Therefore, the approach is dependent on the existence of a variational–preferably a minimum–principle that characterizes the solutions of interest. For conservative systems such as hyperelastic bodies in static equilibrium, the attendant minimum principle is well-known: the stable configurations of the body minimize its potential energy. In problems concerned with dissipative solids, which are the main focus of this paper, the existence of an underlying minimum principle is not immediately obvious. Ortiz *et al.* ([2–5]) have shown that the initial boundary-value problem for a broad class of those dissipative solids can be given a variational structure by recourse to time discretization. For example, any (even highly anisotropic) finite strain plasticity model based on associative evolution equations can be recast into such a variational framework, cf. [20]. Within this variational approach, the solutions of the time-discretized incremental problem are characterized by a minimum principle similar in structure to the principle of minimum potential energy. The requisite effective energy density $W_n(\boldsymbol{F}_{n+1})$ follows from a local relaxation of the internal state [2, 3]. Here, the subindex $n$ refers to a discrete time $t_n$ for which the solution is known, whereas the subindex $n+1$ refers to a subsequent time $t_{n+1}$ at which the solution is sought. The notation is intended to emphasize that the effective energy density $W_n$ varies between time steps, thus allowing for irreversibility, hysteresis and dissipation. The fundamental property of the effective energy density [2, 3] is that it supplies a potential for the incremental stress-deformation relations, i. e.,

$$\boldsymbol{P}_{n+1} = \frac{\partial W_n}{\partial \boldsymbol{F}_{n+1}}(\boldsymbol{F}_{n+1}) \tag{1}$$

where $\boldsymbol{F} := \mathrm{GRAD}\boldsymbol{\varphi}$ is the deformation gradient and $\boldsymbol{P}$ is the first Piola-Kirchhoff stress tensor. Similarly to hyperelasticity, the existence of an effective energy density allows the introduction of the incremental potential energy

$$I_n(\boldsymbol{\varphi}_{n+1}) := \int_\Omega W_n(\mathrm{GRAD}\boldsymbol{\varphi}_{n+1})\,\mathrm{d}V - \int_\Omega \boldsymbol{B}_{n+1}\cdot\boldsymbol{\varphi}_{n+1}\,\mathrm{d}V - \int_{\partial\Omega_2} \bar{\boldsymbol{T}}_{n+1}\cdot\boldsymbol{\varphi}_{n+1}\,\mathrm{d}A\,, \tag{2}$$

where $\Omega$ is the domain occupied by the body in its undeformed configuration, $\boldsymbol{B}$ are the body forces and $\bar{\boldsymbol{T}}$ are the tractions applied over the traction boundary $\partial\Omega_2$. The stable configurations of the solid at time $t_{n+1}$ then follow from the incremental minimum potential energy principle

$$\begin{array}{c} \inf \\ \boldsymbol{\varphi}_{n+1} \in V, \\ \boldsymbol{\varphi}_{n+1}|_{\partial\Omega_1} = \bar{\boldsymbol{\varphi}}_{n+1} \end{array} \qquad I_n(\boldsymbol{\varphi}_{n+1})\,, \tag{3}$$

where $V$ is some suitable space of functions, $\boldsymbol{\varphi}$ is the deformation mapping, and $\bar{\boldsymbol{\varphi}}$ is the deformation mapping prescribed over the displacement boundary $\partial\Omega_1$. For further applications of these ideas, see also ([6, 7], [8]). A comparison of variational constitutive updates may be found in [26]. The precise form of the constitutive model used in calculations is presented in

Section 4.1. As in the case of hyperelasticity, this minimum principle provides an unambiguous comparison criterion for test functions: a test function $\boldsymbol{\varphi}_{n+1}^{(1)}$ is *better* than another $\boldsymbol{\varphi}_{n+1}^{(2)}$ if *and only if* $I_n(\boldsymbol{\varphi}_{n+1}^{(1)}) < I_n(\boldsymbol{\varphi}_{n+1}^{(2)})$. This comparison criterion in turn provides a suitable basis for variational adaptivity in problems involving dissipative materials.

# 3 MESH REFINEMENT AND UNREFINEMENT BY EDGE BISECTION

Throughout this work, mesh refinement is effected by edge-bisection, see [21, 23, 27]. Specifically, we adopt the refinement scheme developed in [1] and depicted in Fig. 1. Edge bisection

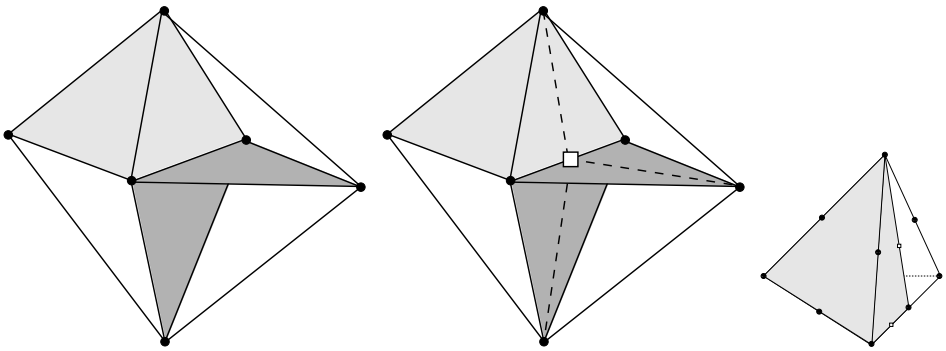


Figure 1: Edge-bisection of simplicial mesh. a) Edge star before bisection. b) Bisection and reconstruction of the star of the bisected edge; □ is the terminal vertex $v$ c) Edge bisection in a 10-node tetrahedral element by using edge bisection. The filled circles represent nodes existing prior to bisection; open squares indicate new nodes inserted as a result of bisection.

has been extensively used for purposes of mesh adaption (cf., e. g., [27–30]). In calculation we use Rivara's backward-longest-edge bisection algorithm [27], which guarantees an upper bound on the aspect ratio of the elements. The refined meshes generated by edge-bisection are automatically conforming and schemes to handle hanging nodes, e. g., by the introduction of transition elements, are not required. More importantly, edge-bisection generates a net of *nested* triangulations $\mathcal{T}_h$ and corresponding finite-dimensional subspaces $V_h$ of $V$ parameterized by a directed set $A$ that records the sequence of edge-bisection operations. The ordering $h_1 < h_2$ signifies that the triangulation $\mathcal{T}_{h_2}$ can be reached from the triangulation $\mathcal{T}_{h_1}$ by a sequence of edge bisections. In particular, $V_{h_1} \subset V_{h_2}$ holds and, consequently, $\inf_{V_{h_2}} I_n \leq \inf_{V_{h_1}} I_n$, with the result that edge-bisection guarantees a reduction in the incremental potential energy.

The variationally consistent refinement scheme employed in the present paper is that proposed by [1] (see also [20] for further details). Since the new energy-driven coarsening strategy advocated in this paper is closely related to the refinement strategy in [1], only the new unrefinement method is described in what follows.

## 3.1 Variational unrefinement

The coarsening strategy adopted in this work is to reverse previous edge-bisection steps (cf., e. g., [21, 23, 31] for alternative strategies). In order to make this strategy more precise we introduce the following terminology. Given a vertex $v \in \mathcal{T}_h$, we shall refer to the collection

of simplices in $\mathcal{T}_h$ having $v$ as a face as the *star* of $v$, denoted $\mathrm{St}(v)$. Likewise, given an edge $e \in \mathcal{T}_h$, we shall refer to the collection of simplices in $\mathcal{T}_h$ having $e$ as a face as the *star* of $e$, denoted $\mathrm{St}(e)$. We recall that the bisection of an edge results in the insertion of a new vertex. We shall say that an inserted vertex $v$ is *terminal* if its star $\mathrm{St}(v)$ has not changed after insertion, see Fig. 1b). A terminal vertex $v$ inserted as a result of the bisection of an edge $e$ has the property that its star $\mathrm{St}(v)$ can be deleted, and the star $\mathrm{St}(e)$ of $e$ reinstated, without affecting the remainder of the triangulation.

In order to formalize this notion, let $V(\mathcal{T}_h)$ denote the collection of vertices of $\mathcal{T}_h$ and $V_0(\mathcal{T}_h)$ the collection of terminal vertices. In addition, for a terminal vertex $v \in V_0(\mathcal{T}_h)$ let $\sigma_v : A \to A$ denote a mapping such that $\mathcal{T}_{\sigma_v(h)}$ is the triangulation resulting from the deletion of $v$. Then, we shall say that $\mathcal{T}_h$ is *unrefinement-stable* if

$$\mu(\mathcal{T}_h) = \max_{v \in V_0(\mathcal{T}_h)} \left( \inf I_{\sigma_v(h)} - \inf I_h \right) > \mu_c. \tag{4}$$

The energy $\mu(\mathcal{T}_h)$ may be regarded as the energy cost of inserting the vertex $v$ back into the mesh, or, in analogy with statistical mechanics of open systems of particles, a *chemical potential*. Thus, $\mathcal{T}_h$ is unrefinement-stable, the deletion of one terminal vertex increases $I_h$ at worst by an amount $\mu(\mathcal{T}_h)$ greater than a tolerance $\mu_c$, and thus the deletion is to be rejected. The unrefinement strategy that emerges from these considerations may be summarized as follows:

i) Find $v \in V_0(\mathcal{T}_h)$ for which $\mu(\mathcal{T}_h)$ is attained.

ii) Is $\mu(\mathcal{T}_h) \leq \mu_c$

YES: Reset $h \leftarrow \sigma_v(h)$, GOTO (ii).

NO: EXIT.

It is elementary to show (cf. [1, 20]) that, for linear problems with potential energies of the form

$$I(u) = \frac{1}{2} a(u,u) - f(u) \tag{5}$$

where $a : V \times V \to \mathbb{R}$ is a coercive, symmetric and continuous bilinear form and $f : V \to \mathbb{R}$ is a continuous linear operator, the chemical potential reduces to

$$\mu(\mathcal{T}_h) = ||u_{\sigma_v(h)} - \inf u_h||_E^2 \tag{6}$$

where $u_{\sigma_v(h)}$ and $\inf u_h$ are the minimizers of $I_{\sigma_v(h)}$ and $\inf I_h$, respectively, and $||u||_E^2 = a(u,u)$ is the energy norm. It therefore follows that, for linear problems, the chemical potential measures the energy distance between the original and unrefined discrete solutions. Consequently, the variational unrefinement criterion accepts the unrefined solution provided that it is close enough to the original solution in the energy-norm distance.

The complementary notion of *refinement stability* has been introduced in [1], namely, $\mathcal{T}_h$ is bisection-stable, the bisection of one edge lowers $I_h$ at best by an amount $\mu(\mathcal{T}_h)$ less than $\mu_c$, and thus the bisection is to be rejected. Evidently, variational $h$-refinement and unrefinement can be achieved by requiring that a triangulation be both refinement and unrefinement stable. Stability can be enforced by alternating refinement and unrefinement operations until both the bisection of an edge and the deletion of a terminal vertex change the energy within the prespecified tolerance (cf, e. g., [32, 33]).

## 3.2 A local unrefinement indicator

A drawback of the aforementioned strategy is that the evaluation of the chemical potential $\mu(\mathcal{T}_h)$ requires global computations and therefore it is costly. An alternative strategy suggested in [1] for mesh refinement consists of constraining the relaxation of the displacement field upon removal of a terminal vertex $x$ to a certain sub-mesh $\mathcal{S}_h(v)$ of $\mathcal{T}_h$, or element *patch*, containing $v$. For instance, $\mathcal{S}_h(v)$ can be chosen to be the ring of elements incident to $v$, i. e., the *star* $\mathrm{St}(v)$. Evidently,

$$\mu_{\mathrm{loc}}(\mathcal{T}_h) = \max_{v\in V_0(\mathcal{T}_h)} \left\{ \inf_{\substack{\boldsymbol{\varphi}\in V,\\ \boldsymbol{\varphi}|_{\partial\Omega_1}=\bar{\boldsymbol{\varphi}},\\ \mathrm{supp}(\boldsymbol{\varphi}-\boldsymbol{\varphi}_h)\subset\mathcal{S}_h(v)}} I_{\sigma_v(h)}(\boldsymbol{\varphi}) - I_h(\boldsymbol{\varphi}_h) \right\} \geq \mu(\mathcal{T}_h) \tag{7}$$

and the local chemical potential $\mu_{\mathrm{loc}}(\mathcal{T}_h)$ represents an upper bound of the global chemical potential $\mu(\mathcal{T}_h)$. In this expression, $\varphi_h$ is a minimizer of $I_h$ and $\mathrm{supp}$ denotes the support of a function. Thus, $\mu_{\mathrm{loc}}(\mathcal{T}_h)$ is computed by constraining the relaxed displacements $\boldsymbol{\varphi}$ on the unrefined mesh $\mathcal{T}_{\sigma_v(h)}$ to differ from the minimizer $\boldsymbol{\varphi}_h$ on the original mesh $\mathcal{T}_h$ only within the neighborhood $\mathcal{S}_h(v)$ of the terminal vertex $v$. Conveniently, this computation is local and its cost is constant independent of the size of the mesh. The resulting $h$-adaption strategy is:

i) Initialize $h = 0$.

ii) Find $v \in V_0(\mathcal{T}_h)$ for which $\mu_{\mathrm{loc}}(\mathcal{T}_h)$ is attained.

ii) Is $\mu_{\mathrm{loc}}(\mathcal{T}_h) \leq \mu_c$

YES: Reset $h \leftarrow \sigma_v(h)$, GOTO (ii).

NO: EXIT.

Locally constrained minimization problems such as defined have also been proposed as a basis for deriving *a posteriori* error bounds in linear problems [34, 35]. Because of the upper bound property $\mu_{\mathrm{loc}}(\mathcal{T}_h) \geq \mu(\mathcal{T}_h)$, the unrefinement criterion based on the local estimate $\mu_{\mathrm{loc}}(\mathcal{T}_h)$ may target meshes for unrefinement that would otherwise be accepted according to the global energy criterion.

## 3.3 Management of history variables

Mesh adaption in problems involving dissipative materials often requires complex remapping procedures for transferring the internal variable set from an initial mesh to a refined triangulation (cf., e. g., [2, 25]). The formulation of remapping procedures is compounded by the presence of internal constraints such as plastic incompressibility. Perhaps the most detrimental aspect of remapping is that it may result in significant numerical diffusion, which can hinder the progression of processes of strain localization and result in overly smooth solutions.

### 3.3.1 Mesh refinement

The process of remapping upon mesh refinement is rendered trivial in the case of bisection of simplicial elements, since in that case the children elements inherit the state of their parent element. In particular, the state of the children elements trivially satisfies all internal constraints and is exactly consistent with the history of deformation of their parent element. Within the present paper, the state variables are assumed to be piecewise constant over the VORONOI cells defined by the quadrature points. Upon bisection, the internal variables are remapped to the new mesh by means of the variational transfer operator of [25]. By the use of piecewise-constant interpolation, the consistent transfer operator according to [25] simplifies greatly. More precisely, the history variables at a newly inserted GAUSS point equal those of the closest old quadrature point.

### 3.3.2 Mesh coarsening

A strategy that also renders remapping trivial upon unrefinement consists of retaining the bisected parent elements in the mesh. These elements do not contribute to the nodal force array but their state is continually updated from the displacement field. It is interesting to note that the deformation that the parent elements experience is an average of the compatible deformations of the children elements and that their state reflects the evolution of the internal state of the material under that average deformation. When a terminal vertex is deleted, the parent elements that are exposed become newly active and have up-to-date internal states. Again, the state of the newly active elements trivially satisfies all internal constraints and is exactly consistent with the history of deformation of those elements and the average history of deformation of the deleted children elements.

# 4 NUMERICAL EXAMPLES

In this section, the performance of the proposed $h$-adaption is demonstrated by means of the test case of a notched finitely-deforming elastic and elastic-plastic specimens, Fig. 2. In order to test the refinement/unrefinement strategy, after some initial loading the crack length is suddenly increased. This causes the mesh around the initial crack front to unrefine and a new refined mesh to become established around the new crack tip. If the size of the problem is kept roughly constant, e. g., at machine capacity, this process may be regarded as a transfer of nodes from the initial to the subsequent crack front. For an elastic material, this transfer is complete and the initial crack front is completely unrefined, with no memory of its former presence remaining in the mesh. By way of sharp contrast, for an elastic-plastic material a state of residual stress remains in the vicinity of the first crack front, which is strongly plastically deformed during loading. This state of residual stress must be resolved with sufficient accuracy throughout the subsequent history of the specimen, and a competition for mesh resolution between the initial and the subsequent crack fronts ensues. Evidently, the optimum distribution of resources between the crack fronts is difficult to strike on a purely *ad hoc* basis. As we shall see, the variational approach effectively supplies an optimal solution to the problem.

In view of the symmetries of the problem the analysis is restricted to one eighth of the specimen. All calculations are carried out using 10-node tetrahedral elements. The amplitude of the prescribed displacement field is $u = 0.16$m and the length of the crack is $l_{\mathrm{c}} = 1.0$m. Following [34, 36] we adopt the following criteria for selecting edges and vertices for refinement and

unrefinement:

$$\text{bisect edge } e \text{ if } \mu_{\rm loc}(e) > \alpha\ \mu_{\rm loc}(\mathcal{T}_h) \tag{8a}$$

$$\text{delete terminal vertex } v \text{ if } \mu_{\rm loc}(v) < \beta\ \mu_{\rm loc}(\mathcal{T}_h) \tag{8b}$$

where $\mu_{\rm loc}(e)$ and $\mu_{\rm loc}(v)$ are the energy release associated with bisecting edge $e$ (cf. [1, 20]) and the energy costs of deleting the terminal vertex $v$ (see Eq. (7)), respectively. In calculations we chose $\alpha = 0.5$ and $\beta = 0.01$.

## 4.1 Constitutive model

In calculations we assume a Helmholtz free-energy function of the form

$$W(\boldsymbol{F}, \boldsymbol{F}^{\rm p}, \varepsilon^{\rm p}) = W^{\rm e}(\boldsymbol{F} \cdot \boldsymbol{F}^{{\rm p}-1}) + W^{\rm p}(\varepsilon^{\rm p}) \tag{9}$$

Here, $W^{\rm e}$ denotes the elastic free energy and $W^{\rm p}$ represents the stored energy due to plastic work of the material, which is assumed to be isotropic. Following Ortiz *et al.*, cf. [2, 3] a finite-deformation variational formulation of von Mises plasticity is obtained by postulating the flow rule

$$\dot{\boldsymbol{F}}^{\rm p} \cdot \boldsymbol{F}^{{\rm p}^{-1}} = \dot{\varepsilon}^{\rm p}\ \boldsymbol{M}, \quad {\rm tr}(\boldsymbol{M}) = 0, \quad \frac{2}{3}\ \boldsymbol{M} : \boldsymbol{M} = 1, \quad \dot{\varepsilon}^{\rm p} \geq 0 \tag{10}$$

where the unknown tensor $\boldsymbol{M}$ defines the direction of plastic flow and the labels $n$ and $n+1$ refer to the discrete times $t_n$ and $t_{n+1}$, respectively. This flow rule may be discretized in time by recourse to the exponential mapping ([3, 37], [2]), with the result

$$\boldsymbol{F}^{\rm p}_{n+1} = \exp[\Delta\varepsilon^{\rm p}\ \boldsymbol{M}] \cdot \boldsymbol{F}^{\rm p}_n \tag{11}$$

The elastic energy density is assumed to be of Hencky-type

$$W(\boldsymbol{F}) = \frac{1}{2}\ \lambda\ \left[\varepsilon_1 + \varepsilon_2 + \varepsilon_3\right]^2 + \mu\ \left[(\varepsilon_1)^2 + (\varepsilon_2)^2 + (\varepsilon_3)^2\right], \quad \varepsilon_i := \log \lambda_i \tag{12}$$

where $\lambda$ and $\mu$ are Lamé constants and $\lambda_i$ are the principal stretches. Plastic work of the material is modeled by means of a standard power-law of the form (cf., e. g., [37], [3])

$$W^{\rm p}(\varepsilon^{\rm p}) = \frac{n\sigma_0\varepsilon^{\rm p}_0}{n+1}\ \left[1 + \left(\frac{\varepsilon^{\rm p}}{\varepsilon^{\rm p}_0}\right)\right]^{(n+1)/n} \tag{13}$$

where $\varepsilon^{\rm p}$ is the effective von Mises plastic strain; $\sigma_0$ is a flow stress; $\varepsilon^{\rm p}_0$ is a reference effective plastic strain; and $n$ is the hardening exponent. The material parameters used in calculations are summarized in Table 1. As noted in Section 2, variational updates enable the time-discretized

| $\lambda$ (N/m$^2$) | $\mu$ (N/m$^2$) | $\sigma_0$ (kN/m$^2$) | $\varepsilon^{\rm p}_0$ | $n$ |
|---|---|---|---|---|
| 115.38 | 76.92 | 1.0 | $0.5 \cdot 10^{-3}$ | 10 |

Table 1: Power-law hardening. Material constants used in calculations.

incremental elastic-plastic problem to be expressed as a minimum problem [2, 3]. Neglecting viscosity and rate effects, the attendant incremental strain-energy density $W_n$ for the preceding model results from the minimization problem

$$W_n(\boldsymbol{F}) = \inf_{\varepsilon^{\rm p}_{n+1}, \boldsymbol{M}} W(\boldsymbol{F}, \boldsymbol{F}^{\rm p}_n, \varepsilon^{\rm p}_{n+1}, \boldsymbol{M}) \tag{14}$$

subject to the constraints (10).

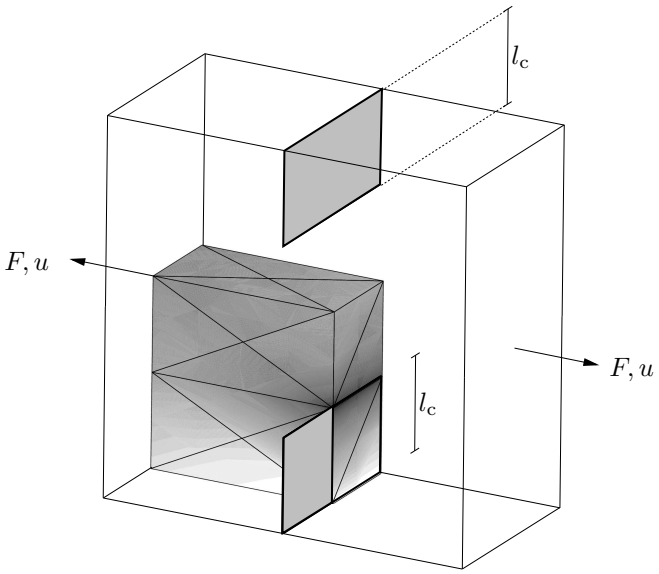


Figure 2: Geometry of the three-dimensional specimen undergoing large deformations. The size of the specimen is $4\text{m}\times4\text{m}\times2\text{m}$ and the initial crack length is $l_c = 1.0\text{m}$. The distribution of the energy density for a Hencky-type material is shown for one octant of the specimen considered in the calculations.

## 4.2 Notched specimen: Hyperelasticity

Fig. 3 shows results obtained from three different finite element analyses using the hyperelastic Hencky model (12): an initial coarse mesh, a uniformly refined mesh and variational $h$-adaption. The initial coarse mesh is shown in Fig. 2. The refinement/unrefinement criteria (8) are applied 18 times. As can be seen from Fig. 3, at first loading $h$-adaption captures the highly localized energy distribution and the resulting deformation better than the uniformly refined triangulations. This improvement can be quantified by means of the computed energies: uniform refinement results in an energy reduction of $0.8\%$, whereas $h$-adaption results in an energy reduction of $1.6\%$ with only one fourth the number of degrees of freedom compared to the uniformly refined mesh.

Next, the crack length is increased from $l_c = 1.0\text{m}$ to $l_c = 1.5\text{m}$ while keeping the prescribed front displacement constant ($u = 0.16\text{m}$), Fig. 4. The figure shows that the variational adaption completely unrefines the fine mesh in the vicinity of the initial crack front and reestablishes it around the subsequent crack front. This requires several coarsening steps in the vicinity of the initial crack front and mesh refinement at the subsequent crack. This is accomplished by applying the refinement/unrefinement criteria (8) 18 times following crack extension. Again, the improvement can be quantified by means of the computed energies: uniform refinement results in an energy reduction of $2.0\%$, whereas $h$-adaption results in an energy reduction of $3.2\%$ with only one half the number of degrees of freedom compared to the uniformly refined mesh.

The preceding energy measures show that variational adaption vastly out-performs uniform refinement, as expected. In interpreting these energy measures it should be carefully born in mind that most of the energy of the specimen is contained in the region away from the crack tip, where the deformations are nearly uniform and, therefore, well-represented by a coarse mesh. This mesh-insensitive component swamps the total energy of the specimen, with the result that the energy reduction due to adaption appears deceptively small. However, the effect of mesh adaption in the vicinity of the crack tip is vastly more pronounced in absolute terms, as attested

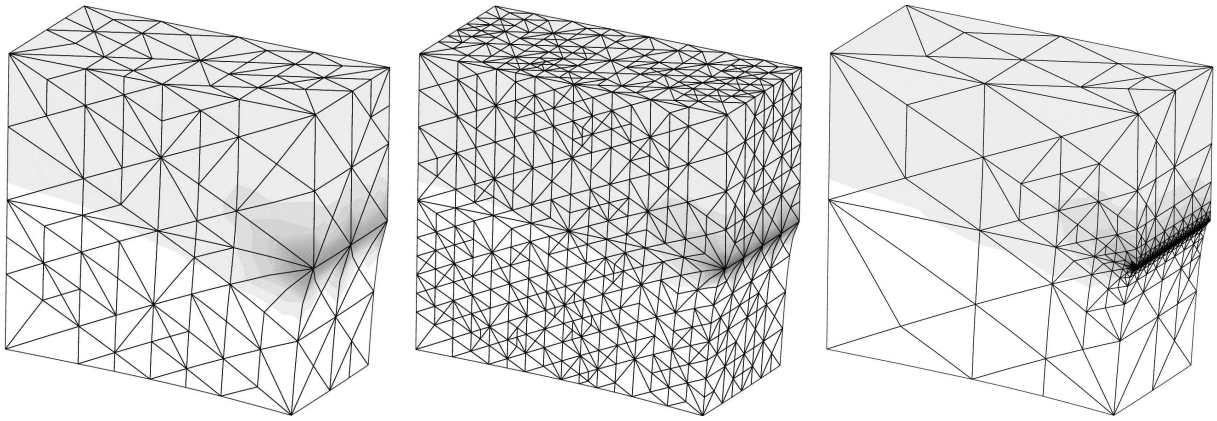

(a) (b) (c)

Figure 3: Hyperelastic three-dimensional specimen undergoing large deformations; crack length $l_{\mathrm{c}} = 1.0$m; $u = 0.16$m. Computed deformed configurations and distribution of the energy density. a) uniformly refined mesh (3179 nodes). b) uniformly refined mesh (39416 nodes). c) proposed $h$-adaption (10052 nodes).

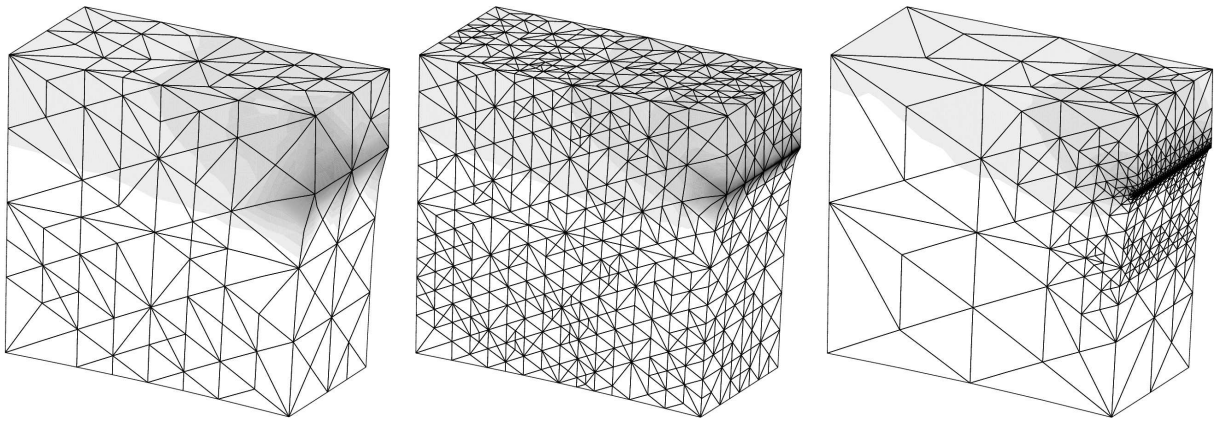

(a) (b) (c)

Figure 4: Hyperelastic three-dimensional specimen undergoing large deformations; crack length $l_{\mathrm{c}} = 1.5$m; $u = 0.16$m. Computed deformed configurations and distribution of the energy density. a) uniformly refined mesh (3179 nodes). b) uniformly refined mesh (39416 nodes). c) proposed $h$-adaption (17902 nodes).

by the radical reconstruction of the mesh in that region.

## 4.3 Notched specimen: Elastic-plastic material response

Finally, we repeat the preceding analysis for an elastic-plastic material. Again, the refinement/unrefinement criteria (8) are applied 18 times following first loading, and three different finite element analyses are compared: an initial coarse mesh, a uniform refinement and variational $h$-adaption. The calculated deformed configurations and the distribution of effective plastic strain are shown in Fig. 5. As in the hyperelastic case, variational $h$-adaption vastly outperforms uniform refinement in terms of energy measure and in mesh resolution near the crack front, where the latter results in a fine graded mesh and a finely resolved effective plastic strain field.

However, a marked difference in behavior with respect to the hyperelastic case occurs upon crack extension, Fig. 7. Unlike the hyperelastic case, owing to the need to resolve the permanent

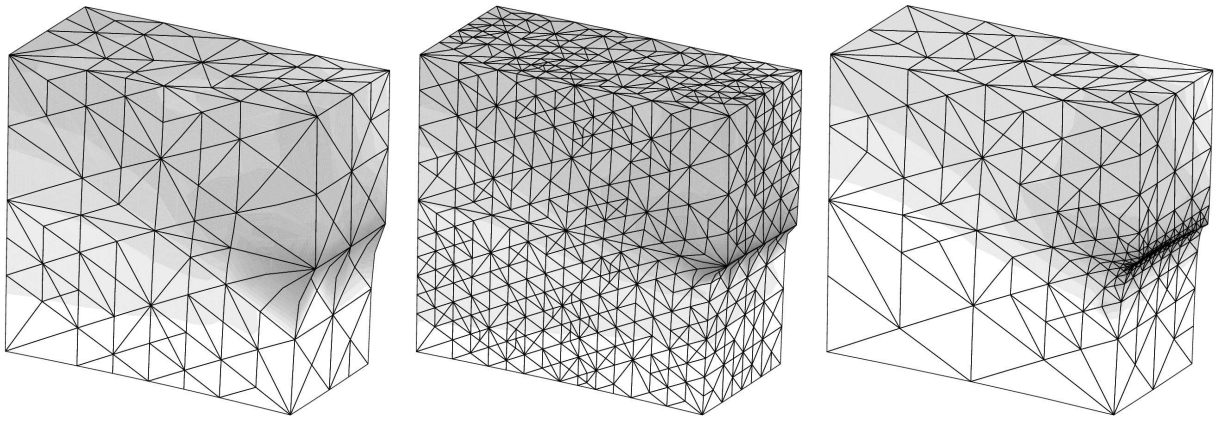

(a) (b) (c)

Figure 5: Hyperelastic-plastic three-dimensional specimen undergoing large deformations; crack length $l_{\mathrm{c}} = 1.0$m; $u = 0.16$m. Computed deformed configurations and distribution of effective plastic strain $\varepsilon^{\mathrm{p}}$. a) uniformly refined mesh (3179 nodes). b) uniformly refined mesh (39416 nodes). c) proposed $h$-adaption (8772 nodes).

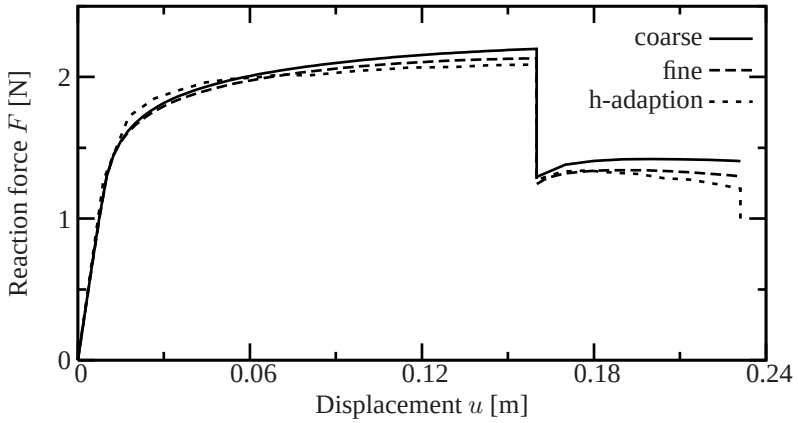


Figure 6: Hyperelastic-plastic three-dimensional specimen undergoing large deformations. Crack length increases from $l_{\mathrm{c}} = 1.0$m up to $l_{\mathrm{c}} = 1.5$m at a front face displacement of $u = 0.16$m. Load-displacement diagrams obtained from: two uniformly refined meshes (coarse and fine); and the proposed variational $h$-adaption.

residual stress field, a fine mesh remains in the vicinity of the initial crack front, though somewhat unrefined relative to the mesh that follows first loading. Simultaneously, a new fine mesh is established around the subsequent crack front. These two demands on resolution, namely, the residual field around the initial crack front and the subsequent crack front, set up a competition for resources, with variational $h$-adaption supplying the optimum compromise. The resulting force-displacement response of the specimen is more compliant than otherwise predicted by the coarse and uniformly refined meshes, Fig. 6. Another numerical example can be found in [20].

# 5 SUMMARY AND CONCLUDING REMARKS

We have developed a variational $h$-adaptive finite element formulation whose distinguishing feature is that mesh refinement and coarsening are governed by the same minimization principle characterizing the underlying physical problem. Hence, no error estimates are invoked at any stage of the adaption procedure. In particular, linearity of the problem and a corresponding

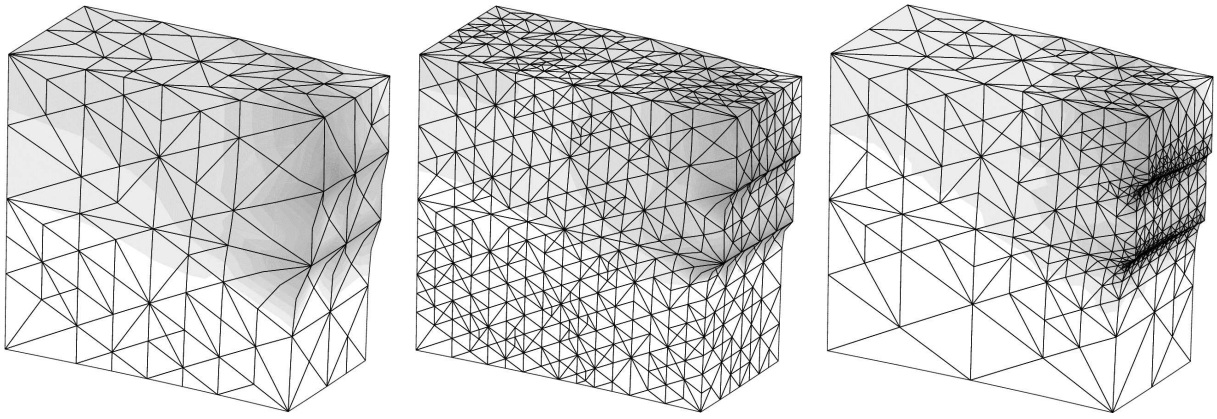

(a) (b) (c)

Figure 7: Hyperelastic-plastic three-dimensional specimen undergoing large deformations; crack length $l_{\mathrm{c}} = 1.5\mathrm{m}$; $u = 0.23\mathrm{m}$. Computed deformed configurations and distribution of effective plastic strain $\varepsilon^{\mathrm{p}}$. a) uniformly refined mesh (3179 nodes). b) uniformly refined mesh (39416 nodes). c) proposed $h$-adaption (19116 nodes).

Hilbert-space functional framework are not required and the proposed formulation can be applied to highly nonlinear phenomena, as demonstrated by numerical examples concerned with finitely-deforming elastic-plastic materials. In this case, and in other similar cases involving inelastic behavior, the requisite minimum principle is supplied by time discretization and the use of variational state updates. The basic $h$-adaption strategy is to refine (respectively, unrefine) the spatial discretization locally if such refinement (respectively, unrefinement) results in a sufficiently large reduction (respectively, sufficiently small increase) in the energy. By estimating the energy variations from local patches, this strategy leads to an adaption algorithm having $O(N)$ complexity. In the particular scheme presented in this paper, local refinement is effected by edge bisection and local unrefinement by the deletion of terminal vertices. In addition, the entire hierarchy of successive refinements is stored and the internal state of parent elements is updated so that no mesh-transfer operator is required upon unrefinement. The versatility and robustness of the variational $h$-adaption scheme have been illustrated in the case of notched specimens with stationary and extending cracks.

The ability of the scheme to adapt the mesh in order to resolve the elastic-plastic crack-front fields and to arbitrate competing demands for resolution from different features of the solution is remarkable. Since both the solution and the adaption procedure are governed by the same physical principle, the solutions supplied by the variational $h$-adaption scheme represent an optimal utilization of fixed computational resources, e. g., as set by machine capacity. In comparison to variational $r$-adaption, variational $h$-adaption combining both refinement and unrefinement is advantageous in that mesh entanglement and topological transitions, or mesh reconnection, are not a concern. Those limitations of variational $r$-adaption can be overcome by combining it with edge flips and other mesh-improvement schemes [15, 16], but such extensions add considerably to the complexity of the implementation. An appealing possibility that uses both approaches synergistically is to implement variational $r$-adaption on top of variational $h$-adaption, and rely on the latter to effectively account for transitions in mesh topology. Early experiments with variational $hp$-adaption [19] demonstrate that $r$-adaptivity indeed provides an additional boost to $h$-adaptive schemes at minimal additional complexity.

# ACKNOWLEDGMENT

Support from the DoE through Caltech's ASC/ASAP Center for the Simulation of the Dynamic Response of Solids is gratefully acknowledged. JM is also grateful for support from the Deutsche Forschungsgemeinschaft (DFG) under contract/grant number: Mo 1389/1-1.

# References

[1] J. Mosler and M. Ortiz. Variational $h$-adaption in finite deformation elasticity and plasticity. *International Journal for Numerical Methods in Engineering*, 2006. accepted.

[2] R. Radovitzky and M. Ortiz. Error estimation and adaptive meshing in strongly nonlinear dynamic problems. *Computer Methods in Applied Mechanics and Engineering*, 172:203–240, 1999.

[3] M. Ortiz and L. Stainier. The variational formulation of viscoplastic constitutive updates. *Computer Methods in Applied Mechanics and Engineering*, 171:419–444, 1999.

[4] M. Ortiz and E.A. Repetto. Nonconvex energy minimisation and dislocation in ductile single crystals. *J. Mech. Phys. Solids*, 47:397–462, 1999.

[5] S. Aubry and M. Ortiz. The mechanics of deformation-induced subgrain-dislocation structures in metallic crystals at large strains. *Proceedings of the Royal Society London A*, 451:3131–3158, 2003.

[6] C. Miehe. Strain-driven homogenization of inelastic microstructures and composites based on an incremental variational formulation. *International Journal for Numerical Methods in Engineering*, 55:1285–1322, 2002.

[7] C. Carstensen, K. Hackl, and A. Mielke. Non-convex potentials and microstructures in finite-strain plasticity. *Proc. R. Soc. Lond. A*, 458:299–317, 2002.

[8] Q. Yang, L. Stainier, and M. Ortiz. A variational formulation of the coupled thermo-mechanical boundary-value problem for general dissipative solids. *Journal of the Mechanics and Physics of Solids*, 54:401–424, 2006.

[9] G.M. McNeice and P.V. Marcal. Optimization of finite-element grids based on minumum potential-energy. *Journal of Engineering for Industry-Transactions of the ASME*, 95(1):186–190, 1973.

[10] C. Felippa. Numerical experiments in finite element grid optimization by direct energy search. *Appl. Math. Modelling*, 1:93–96, 1976.

[11] J.D. Eshelby. The force on an elastic singularity. *Phil. Trans. R. Soc. Lond. A*, 244:87–112, 1951.

[12] J.D. Eshelby. The elastic energy-momentum tensor. *J. Elasticity*, 5:321–335, 1975.

[13] M. Braun. Configurational forces induced by finite element discretization,. *Proc. Estonian Acad. Sci. Phys. Math.*, 46:24–31, 1997.

[14] R. Mueller and G.A. Maugin. On material forces and finite element discretizations. *Computational Mechanics*, 29:52–60, 2002.

[15] P. Thoutireddy. *Variational Arbitrary Lagrangian-Eulerian method*. PhD thesis, California Institute of Technology, Pasadena, USA, 2003.

[16] P. Thoutireddy and M. Ortiz. A variational r-adaption and shape-optimization method for finite-deformation elasticity. *International Journal for Numerical Methods in Engineering*, 61:1–21, 2004.

[17] E. Kuhl, H. Askes, and P. Steinmann. An ALE formulation based on spatial and material settings of continuum mechanics. Part 1: Generic hyperelastic formulation. *Computer Methods in Applied Mechanics and Engineering*, 193(39-41):4207–4222, 2004.

[18] H. Askes, E. Kuhl, and P. Steinmann. An ALE formulation based on spatial and material settings of continuum mechanics. Part 2: Classification and applications. *Computer Methods in Applied Mechanics and Engineering*, 193(39-41):4223–4245, 2004.

[19] J. Mosler and M. Ortiz. On the numerical implementation of variational arbitrary lagrangian-eulerian (vale) formulations. *International Journal for Numerical Methods in Engineering*, 2006. (in press).

[20] J. Mosler. *On the numerical modeling of localized material failure at finite strains by means of variational mesh adaption and cohesive elements*. Habilitation, Ruhr University Bochum, Germany, 2007. `www.tm.bi.rub.de/mosler`.

[21] M.-C. Rivara. Local modification of meshes for adaptive and / or multigrid finite-element methods. *Journal of Computational and Applied Mathematics*, 36:79–89, 1991.

[22] M.-C. Rivara and Ch. Levin. A 3-D refinement algorithm suitable for adaptive and multigrid techniques. *Communications in Applied Numerical Methods*, 8:281–290, 1992.

[23] E. Bänsch. Local mesh refinement in 2 and 3 dimensions. *Impact of Computing in Science and Engineering*, 3:181–191, 1991.

[24] J.F. Molinari and M. Ortiz. Three-dimensional adaptive meshing by subdivision and edge-collapse in finite-deformation dynamic plasticity problems with application to adiabatic shear banding. *International Journal for Numerical Methods in Engineering*, 53:1101–1126, 2002.

[25] M. Ortiz and J.J. Quigley. Adaptive mesh refinement in strain localization problems. *Computer Methods in Applied Mechanics and Engineering*, 90:781–804, 1991.

[26] J. Mosler. *On the numerical modeling of localized material failure at finite strains by means of variational mesh adaption and cohesive elements*. Habilitation, Lehrstuhl für Technische Mechanik, Ruhr University Bochum, Germany, 2006. submitted.

[27] M.-C. Rivara. New longest-edge algorithms for the refinement and/or improvement of unstructured triangulations. *International Journal for Numerical Methods in Engineering*, 40:3313–3324, 1997.

[28] W.F. Mitchell. Adaptive refinement for arbitrary finite-element spaces with hirachical bases. *International Journal for Numerical Methods in Engineering*, 40:3313–3324, 1997.

[29] Kossaczký. A recursiv approach to local mesh refinement in two and three dimensions. *Journal of Computational and Applied Mathematics*, 55:275–288, 1994.

[30] J.M. Maubach. Local bisection refinement for N-simplicial grids generated by reflection. *SIAM J. Sci. Comput.*, 16:210–227, 1995.

[31] E. Bänsch. An adaptive finite-element strategy for the three-dimensional time-dependent navier-stokes equations. *Journal of Computational and Applied Mathematics*, 36:3–28, 1991.

[32] A. Schmidt and K.G. Siebert. ALBERT: An adaptive hierarchical
nite element toolbox. Technical report, Institut für Angewandte Mathematik, Albert-Ludwigs-Universität Freiburg, 2000.

[33] A. Ern and J.-L. Guermond. *Theory and practice of finite elements*. Spinger New York, 2004.

[34] R. Verfürth. *A review of a priori error estimation and adaptive mesh-refinement techniques*. Wiley-Teubner, 1996.

[35] M. Ainsworth and J.T. Oden. *A Posterior Error Estimation in Finite Element Analysis*. Wiley, 2000.

[36] O.C. Zienkiewicz, D.W. Kelly, J. Gago, and I. Babuška. Hierarchical finite element approaches, error estimates and adaptive refinement. In J. Whiteman, editor, *The mathematics of finite elements and applications IV*, pages 313–346, 1982.

[37] A. M. Cuitiño and M. Ortiz. A Material-Independent Method for Extending Stress Update Algorithms from Small-Strain Plasticity to Finite Plasticity with Multiplicative Kinematics. *Engineering Computations*, 9:437–451, 1992.